International Journal of Hyperthermia

ISSN: (Print) (Online) Journal homepage: https://www.tandfonline.com/loi/ihyt20

Histological findings in resected leiomyomas following MR-HIFU treatment, single-institution data from seven patients with unfavorable focal therapy

Antti Viitala, Michael Gabriel, Kirsi Joronen, Gaber Komar, Antti Perheentupa, Teija Sainio, Jutta Huvila, Pekka Pikander, Pekka Taimen & Roberto Blanco Sequeiros

To cite this article: Antti Viitala, Michael Gabriel, Kirsi Joronen, Gaber Komar, Antti Perheentupa, Teija Sainio, Jutta Huvila, Pekka Pikander, Pekka Taimen & Roberto Blanco Sequeiros (2023) Histological findings in resected leiomyomas following MR-HIFU treatment, single-institution data from seven patients with unfavorable focal therapy, International Journal of Hyperthermia, 40:1, 2234666, DOI: 10.1080/02656736.2023.2234666

To link to this article: https://doi.org/10.1080/02656736.2023.2234666

INTERNATIONAL JOURNAL OF HYPERTHERMIA
2023, VOL. 40, NO. 1, 2234666
https://doi.org/10.1080/02656736.2023.2234666

Taylor & Francis
Taylor & Francis Group

Histological findings in resected leiomyomas following MR-HIFU treatment, single-institution data from seven patients with unfavorable focal therapy

Antti Viitala[a], Michael Gabriel[b], Kirsi Joronen[c], Gaber Komar[a], Antti Perheentupa[c], Teija Sainio[d], Jutta Huvila[e], Pekka Pikander[e], Pekka Taimen[e] and Roberto Blanco Sequeiros[a]

[a]Department of Radiology, University of Turku and Turku University Hospital, Turku, Finland; [b]Institute of Biomedicine, University of Turku, Turku, Finland; [c]Department of Obstetrics and Gynecology, University of Turku and Turku University Hospital, Turku, Finland; [d]Department of Medical Physics, University of Turku and Turku University Hospital, Turku, Finland; [e]Department of Pathology, University of Turku and Turku University Hospital, Turku, Finland

ABSTRACT

Purpose: Magnetic resonance – high-intensity focused ultrasound (MR-HIFU) is a noninvasive treatment option for symptomatic uterine leiomyomas. Currently, pretreatment MRI is used to assess tissue characteristics and predict the most likely therapeutic response for individual patients. However, these predictions still entail significant uncertainties. The impact of tissue properties on therapeutic outcomes remains poorly understood and detailed knowledge of the histological effects of ultrasound ablation is lacking. Investigating these aspects could aid in optimizing patient selection, enhancing treatment effects and improving treatment outcomes.

Methods and materials: We present seven patients who underwent MR-HIFU treatment for leiomyoma followed by second-line surgical treatment. Tissue samples obtained during the surgery were stained with hematoxylin and eosin, Masson's trichrome and Herovici to evaluate general morphology, fibrosis and collagen deposition of leiomyomas. Immunohistochemical CD31, Ki-67 and MMP-2 stainings were performed to study vascularization, proliferation and matrix metalloproteinase-2 protein expression in leiomyomas, respectively.

Results: The clinical characteristics and radiological findings of the leiomyomas prior to treatment as well as qualitative histological findings after the treatment are presented and discussed in the context of current literature. A tentative model for volume reduction is presented.

Conclusion: These findings provide insights into potential factors contributing to suboptimal therapeutic outcomes and the variability in histological changes following treatment.

ARTICLE HISTORY
Received 10 April 2023
Revised 15 June 2023
Accepted 4 July 2023

KEYWORDS
MR-HIFU; MR-guided high-intensity focused ultrasound; histology; uterine fibroid; leiomyoma

Introduction

Magnetic resonance – high-intensity focused ultrasound (MR-HIFU) is a therapeutic option for symptomatic uterine leiomyomas [1]. During treatment, absorbed ultrasound induces rapid tissue temperature elevation to approximately 60–70 °C. Over the following months, a reduction in leiomyoma volume and symptom improvement have been observed in most but not all cases [2,3]. The underlying mechanisms contributing to shrinkage, or lack thereof, are not fully understood. Although rare, lack of sufficient treatment response is a potential clinical problem and necessitates a second-line treatment. In this paper, we report our observations of such cases. We review existing literature and describe the histological and radiological findings in seven MR-HIFU-treated patients who underwent second-line surgical treatment due to insufficient treatment outcomes.

Characteristics of uterine leiomyomas

Structure and ECM

Uterine leiomyomas are firm, stiff, nodular tumors consisting of smooth muscle cells (SMCs) and extracellular matrices (ECMs) [4]. Leiomyomas have a well-defined outline and are surrounded by a pseudocapsule consisting of compressed muscle fibers [5]. Leiomyomas grow mostly from their periphery, which has more mitosis (during the secretory phase), apoptosis (during the proliferative phase) and a higher blood vessel density than their central parts [5–7].

Leiomyomas have an excessive amount of ECM when compared with myometrium. The ECM of the leiomyoma tissue consists mainly of collagen, fibronectin and proteoglycans. Collagen type I is the most abundant and is expressed in larger quantities compared to the myometrium [8,9]. Compared to the myometrium, collagen fibrils in leiomyomas

CONTACT Antti Viitala antti.j.viitala@gmail.com Department of Radiology, University of Turku and Turku University Hospital, Kiinamyllynkatu 4-8, 20521 Turku, Finland

Supplemental data for this article can be accessed online at https://doi.org/10.1080/02656736.2023.2234666.

are more abundant, shorter, loosely packed and unorganized [4]. Collagen in the leiomyomas is entirely extracellular [4].

Procollagens and other molecules needed to form the ECM are synthesized by cells and secreted into the interstitial space, where they undergo further processing and self-assembly into the ECM. Individual collagen molecules bundle together to form a microfibril, which in turn cross-links to form collagen fibers. Fibronectin binds to collagen, proteoglycans and other ECM components creating a complex scaffold of molecules. Proteoglycans contain highly hydrophilic components that retain water molecules in ECM and contribute to the overall physical structure of tissues. They also provide co-receptors and storage sites for growth factors stored within the ECM [10–12].

Once formed, the ECM is actively remodeled by regulated processes of degradation and regeneration. Excessive amounts of ECM in leiomyomas are apparently caused by both the overproduction of collagen and a decrease in remodeling and breakdown processes. The ECM interacts with SMCs via mechanotransduction; cells' internal cytoskeleton is attached to the ECM by integrin molecules of the cell membrane, through which the cell receives mechanical cues related to environmental conditions such as stretch and pressure. SMCs of leiomyomas appear to have an attenuated response to mechanical stimulus [11–13].

Matrix metalloproteinase (MMP) enzymes are involved in ECM degradation. MMPs are expressed in SMCs in an inactive form and are secreted into the interstitial space where they are activated. Among the various MMPs, the concentration of MMP-2 is significantly higher in leiomyomas. MMP-2 is known to have the widest target molecule spectrum and is involved in the degradation of both native and denatured collagen. When the ECM is degraded by MMPs, growth factor molecules stored within the ECM may be released and able to bind to SMCs, promoting their proliferation [11,12,14].

Growth and development of leiomyoma

Two intertwined processes are involved in the growth of leiomyomas: the formation of excess SMCs and the production of excess ECM. These are understood to be promoted by mechanotransduction, hormonal signaling and growth factors [12].

Despite the above-mentioned molecular similarities, the composition of the leiomyomas varies considerably. This is seen in properties such as the cellularity, stiffness (elasticity), amount of ECM, and density of vasculature [15]. Mechanical stiffness of the leiomyoma appears to correlate with the amount of ECM and how organized the collagen within the ECM is [4]. The mechanical stiffness may also be related to the interstitial fluid influencing the properties of glycosaminoglycans in the ECM [13] or changes in the relative amount of different collagen types [8]. While SMCs respond to hormonal changes, ECM collagen fibrils are not affected by the menstrual cycle [4]. As leiomyomas grow, they undergo degenerative processes such as hyaline degeneration, fatty degeneration, cystic degeneration, myxoid degeneration, hemorrhagic necrosis and calcification [16–18]. After menopause, a reduction in leiomyoma cell size and overall size is generally observed [19].

MRI characteristics

On MRI, T2-hypointense leiomyomas typically have higher collagen content, mass density, stiffness, water content and cellularity [20–22]. T2-hyperintense leiomyomas tend to have higher cellularity with little collagen or extensive degenerative changes [22,23]. An increase in T2 intensity also correlated with higher proliferative activity [24]. Degenerated leiomyomas tend to have a heterogeneous appearance [16,20,23].

In T1w gadolinium-enhanced MRI (T1gd+), cellular leiomyomas tend to show homogeneity and high enhancement at 30–90 s, whereas degenerated leiomyomas tend to show irregular, peripheral or minimal enhancement. 'Ordinary' leiomyoma showed irregular, peripheral or minimal enhancement while areas with extensive hyaline degeneration show low enhancement [25].

Ultrasound ablation

Acoustic energy transmitted via ultrasound waves is absorbed by the tissue and transformed into thermal energy, thereby inducing rapid local temperature elevation. Histologically, reported changes include coagulation necrosis, hemorrhagic necrosis and hemorrhage [26,27]. For other tissue types such as the liver, thermal fixation [28–31], boiling or cavitation, and collapse of tissue architecture have been reported, especially at higher ultrasound intensities. When the resected leiomyomas were ablated *ex vivo*, coagulation necrosis with preserved tissue architecture was observed in the ablated areas [32].

Radiologically, post-treatment non-perfused volume (NPV) is generally observed [2,33]. Post-treatment NPV often exceeds the ablated area, perhaps owing to the spread of apoptotic mediators [2,27], interruption of vascular supply [27] and underestimation of the extent of thermal dose.

Coagulation necrosis

Traditional morphological characteristics of tissue necrosis include an increase in cell volume, swelling of organelles, and rupture of cell membranes, leading to the loss of intracellular contents [34]. Coagulative necrosis may occur as a result of heating or ischemic injuries.

Thermal fixation

Thermal fixation of heated tissue has been reported in the liver parenchyma [29,30], prostate gland [28] and myometrium [35], suggesting that it could occur in HIFU-treated leiomyoma. Thermal fixation tends to occur in regions receiving higher thermal doses than in areas that undergo coagulation necrosis [30,35]. Thermal-fixed tissue is characterized by cell death combined with preservation of tissue architecture and nuclei [29,30,35]. Nuclei preservation is likely a consequence of the hyperthermic inactivation of intracellular enzymes participating in normal breakdown processes.

Thermally fixed regions appear to resist normal tissue breakdown, perhaps secondary to the thermal denaturation of proteins, which might lead to foreign body reactions. Reabsorption of tissue debris is inhibited, and a giant cell reaction can be observed at the periphery of the zone. Cellular staining properties of thermally fixed tissue have been reported to fade over time, while tissue architecture is preserved, resulting in characteristics mimicking coagulative necrosis [35].

Thermal changes in collagen

As the ECM is heated, denaturation of collagen is feasible at temperatures and time spans encountered during MR-HIFU [10]. Some changes in the collagen structure may be reversible, but at higher temperatures irreversible changes occur [10]. The denaturation rate is known to depend on temperature, mechanical load, hydration, chemical environment and amount of cross-linking (maturity) [10]. *Ex vivo* bovine tendons, which have high collagen content, shrink when heated [36]. The amount of shrinkage depends on the temperature and exposure time, while the proportion of denatured collagen fibrils increases with shrinkage [36]. Despite the initial shrinking, heat-treated tendons lose their mechanical strength and become easier to stretch [36]. Typical shrinkage temperature of mammalian collagens is known to be around 65–67 °C [37].

Vessel occlusion

Intentional targeting of the main arteries of leiomyomas is technically viable, resulting in devascularization extending much further than the original ablated area [38]. Even without intentional targeting, NPV is routinely observed to extend beyond the targeted volume. Pathological features in the ischemic area should resemble those encountered following uterine artery embolization (UAE), namely necrosis, calcification and vascular thrombosis [39].

Ultrasound ablation: delayed effects

In an early trial, when seven patients underwent hysterectomy within one month of treatment, pathological findings included coagulative necrosis and hemorrhage [27,40]. In a series of 12 patients who underwent second-line surgical treatment at a median time of seven months, the most common histological finding was infarction-type necrosis surrounded by granulation tissue, concomitant with the infiltration of lymphocytes and macrophages [41]. It has been proposed that either apoptosis mediators or their impact on the local vasculature could spread and extend the initial area of necrosis [2,27,33]. Changes in mechanotransduction-mediated signaling or the hormonal environment also seem feasible.

Leiomyoma shrinkage

Most leiomyoma volume reduction occurs during the first six months, followed by slower volume reduction over the next few years [2,3]. At six months, the volume of the NPV is reported to shrink by approximately 70% regardless of the T2 intensity of the leiomyoma tissue. While in the remaining perfusing part of the leiomyoma, the volumetric change is reported to range from −25% (T2-hypointense tissue) to +42% (T2-hyperintense tissue) [2].

There is still a poor understanding of the processes, which contribute to the shrinkage of leiomyomas. Hypotheses presented so far include apoptosis [33], phagocytosis [33], breakdown and absorption of necrotic tissue [42], healing of the thermal injury [33], replacement of necrotic tissue with other tissue types such as granulation and scar tissue, changes in local hormonal activity, immunological response, changes in local vasculature, or a combination of multiple processes. One of our aims was to add to the limited data available on these processes. Despite shrinkage, some residual NPV usually remains *in situ* months after treatment, and possibly permanently [42].

Materials and methods

Potential candidates were referred from hospitals around Finland and recruited for the ongoing clinical trial (NCT02914704). Ethics approval was obtained from the Hospital District Ethics Committee (approval # ETMK:95/1801/2015 16.6.2015). The patients underwent screening by a gynecologist, followed by MRI. A multidisciplinary team discussed each treatment decision. Informed consent was obtained from all the participants. Therapies were conducted using the Profound Medical Sonalleve V2 MR-HIFU device (SW version 3.5.1271.1817) on a Philips Ingenia 3.0T MR system. Patients were followed up through gynecology visits, symptom severity score questionnaires, and MRI.

In the cases reported here, surgical intervention was selected as the second-line treatment (Table 1) and included two myomectomies and five hysterectomies (two by morcellation). Myomectomy or hysterectomy specimens were placed in formalin in the operating room and embedded in paraffin after 24 h fixation. Tissue sections were cut at 5 μm thickness. Initial staining was performed using either Van Gieson's or hematoxylin and eosin (H&E) staining. After identifying the relevant samples, further staining was performed with H&E, Masson's trichrome (MTri) and Herovici. Immunohistochemical staining was performed using CD31, Mib-1 and MMP-2 antigens. Details of the staining protocol are given in the supplementary material.

Histological slides were digitized using a 3DHISTECH Pannoramic 250 scanner (3DHISTECH Ltd., Budapest, Hungary). Image analysis was conducted using the QuPath v.0.2.0m8 [43]. QuPath's cell detection functionality was used to calculate the number of cell nuclei per mm^2 (cell density, CD), which was used to identify the pixels containing extracellular collagen from MTri staining and pixels containing CD31+ cells. The proportion of these areas compared to the overall surface area was calculated (collagen%, CD31%). While platelets and some immune cells are CD31-positive, the majority of CD31+ cells are endothelial cells lining blood

Table 1. Patient characteristics.

	Age	Myoma	Funaki (T2) classification	Mindjuk (T1gd+) classification	Symptoms	Medication
Case 1	46 y	898 ml Submucosal	Type II, homogeneous	Type II, heterogeneous	Pain and pressure at lower abdomen	–
Case 2	38 y	95 ml Subserosal	Type II, homogeneous	Type III, heterogeneous	Abdominal pressure, urinary frequency	–
Case 3	32 y	21 ml Intramural	Type II, heterogeneous	Type III, homogeneous	Infertility, deformation of the uterine cavity due to leiomyoma	Ulipristal acetate prior HIFU
Case 4	40 y	59 ml Intramural	Type II, homogeneous	Type II homogeneous (venous phase) Type III homogeneous (arterial phase)	Hypermenorrhea leading to anemia	Combined oral contraceptive post HIFU
Case 5	41 y	242 ml Intramural	Type II, homogeneous	Type II, homogeneous	Hypermenorrhea, urinary urgency	Ulipristal acetate prior HIFU, hormonal IUD prior and post HIFU
Case 6	38 y	170 ml Intramural	Type II, homogeneous	Type III, homogeneous	Hypermenorrhea	Ulipristal acetate prior HIFU
Case 7	41 y	361 ml Intramural	Type II, homogeneous	Type II, homogeneous	Urinary frequency	Ulipristal acetate post HIFU

vessels. Therefore, CD31% was used as an indication of histologically confirmed vasculature.

MRI characteristics on T2 were categorized according to the Funaki classification [33] and T1gd + according to the classification described by Mindjuk et al. [44].

Results

Patient characteristics and procedural outcomes

Although all treated myomas were Funaki type II, there were considerable variations in their gadolinium uptake, CD, collagen% and CD31% (Figure 1, Table 1). The median non-perfused volume percentage (NPV%) immediately post-treatment was 37% (Table 2). No HIFU-related complications occurred in any of the patients. Median tumor shrinkage confirmed by MRI at the time of surgery was 31%. The reasons for second-line surgical treatment included insufficient clinical symptom improvement ($N = 6$), the appearance of new leiomyoma ($N = 1$) and low initial NPV% ($N = 1$).

Cases without histologically confirmed necrosis

Case 1

A large leiomyoma (848 ml) showed heterogeneity in the pretreatment T1gd + image. Owing to poor heating, the patient underwent two HIFU treatments, resulting in an NPV% of 37% and a leiomyoma volume reduction of 9% at three months. As the clinical response was insufficient, laparoscopic hysterectomy was performed at 13 months. In the gross pathology section, leiomyoma was soft and disintegrated, containing a cavity filled with a gel-like substance. Histologically, tissue structure degeneration was observed at the rim of the liquefied cavity while no necrotic areas were observed (Figure S1).

Case 2

Although the tissue heated well, the NPV% was only 9% owing to anatomical constraints. A shrinkage of 48% and complete disappearance of the NPV were observed at six months. Hysterectomy was performed due to insufficient clinical improvement. No necrotic areas or other tissue changes were identified in the histological samples (Figure S2).

Case 4

The patient had a single 59 ml intramuscular leiomyoma. In T1gd+, the myoma was hyperintense to the myometrium during the arterial phase and hypointense during the venous phase, indicating very rapid gadolinium wash-in and wash--out. The heating was poor. Based on simulations, high perfusion and the deep location of the myoma were identified as the most plausible explanations for poor heating [45]. At post-treatment T1gd+, a good NPV% was observed during the arterial phase, which then decreased to a minimum of 3% during 10-min dynamic scanning. Hysterectomy was performed at one month. In the gross pathology section, the leiomyoma tissue appeared hemorrhagic. The tissue was highly cellular, highly vascularized and contained practically no collagen (Figure S4).

Cases with histologically confirmed necrosis

Histological necrosis corresponding to the treated regions was observed in four cases (cases 3, 5, 6 and 7). In each case, we observed regions of dense scarred tissue, consisting of highly organized collagen bundles mixed sparsely with basophilic nuclei (Figure 2(a)). Sparse Mib-1+ and MMP-2+ cells were observed in the collagenous material. In case 7, few blood vessels were observed within the dense scarred tissue region. In all cases, the scarred region shared a boundary with remaining leiomyoma tissue (Figure 3).

In cases 3 and 5, we observed a central region of non-organized coagulative necrosis (Figure 2(b)). These regions were characterized by preserved tissue architecture, that is, EMC with empty cell compartments of approximately the same size as the cells in the surrounding leiomyoma tissue, and unorganized collagen bundles roughly corresponding to the size and shape of the collagen bundles of the surrounding leiomyoma tissue. Hematoidin deposits were present, indicating that hemoglobin had undergone metabolism under low-oxygen conditions. Remnants of blood vessels

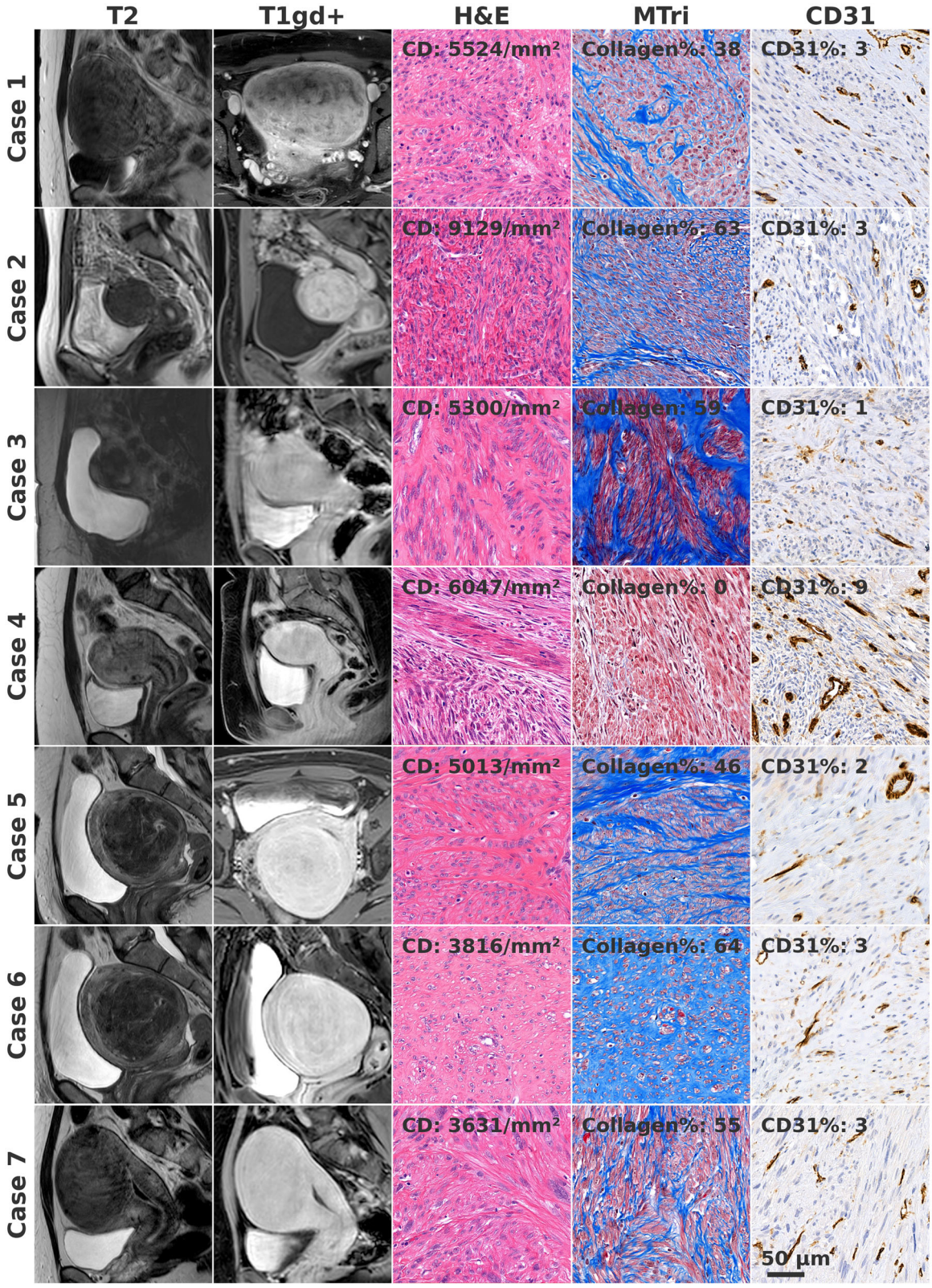

Figure 1. Pretreatment MR-images. Histological samples are from the regions of the remaining leiomyoma tissue. CD: collagen% and CD31% show heterogeneous histology. Scale bar applies for all histological images.

lined with CD31+ endothelial cells were also present. Mib-1+ and MMP-2+ cells were not detected. In both cases, regions with non-organized coagulative necrosis shared a boundary with the dense scarred regions, which in turn shared a boundary with remaining leiomyoma tissue. In case 3, the dense collagenous area was organized as a one to four mm thick scar-like rim surrounding the central area of coagulative necrosis (Figure S3), at the periphery of the heating effect. For other cases, the maximal thicknesses of the dense scarred regions on histology slides were 10, 9 and 3 mm.

Table 2. Procedural outcomes.

	HIFU procedure	Initial NPV	Leiomyoma volume change post-therapy	Reason for surgery	Surgery
Case 1	Poor tissue heating at therapy time, response varied at different areas	37% (after two HIFU procedures)	−9% at 3 months	Insufficient clinical response	13 months post HIFU, laparoscopic hysterectomy
Case 2	NPV limited by surrounding bowel loops	9%	−48% at 6 months	Insufficient clinical response	7 months post HIFU, hysterectomy
Case 3	Heats well	36%	−38% at 10 months	Continued uterine cavity deformation and infertility, appearance of new leiomyomata	10 months post HIFU, laparoscopic myomectomy
Case 4	Highly vascularized leiomyoma, poor heating despite using maximum power 300 W	3%	Follow-up imaging not done	Low NPV	1 months post HIFU, hysterectomy
Case 5		50%	−24% at 12 months	Insufficient clinical response	29 months post HIFU, laparoscopic hysterectomy using morcellation
Case 6	Heats well	54%	−22% at 3 months	Insufficient clinical response	19 months post HIFU, laparoscopic myomectomy
Case 7		45%	−42% at 3 months	Symptom recurrence at one year	16 months post HIFU, laparoscopic hysterectomy with morcellation

Boundary area

For cases 3 and 6, the transition between collagenous tissue type and untreated leiomyoma tissue was sharp (Figure 3). In cases 5 and 7, a transition layer (approximate width 0.4 mm) was observed, which was characterized by a decreased density of myocytes and increased collagen. No increase in Mib-1+, CD31+ or MMP-2+ cells was observed at the boundary. In Herovici staining, collagen appeared to be mature. In case 3, few macrophages and lymphocytes were observed close to the boundary. No foreign body or giant cell reaction was observed in any case.

Discussion

In the present study, we report on the histological and radiological findings of seven HIFU-treated leiomyomas with insufficient primary outcomes leading to second-line surgical treatment. The median post-treatment NPV% of reported cases was lower than those typical for HIFU patients at our clinic [46], which is consistent with findings that the re-intervention rate increases when NPV% decreases [42]. Histological samples of remaining leiomyoma tissue after treatment had heterogeneous characteristics. In particular, the collagen% varied considerably between patients, which could impact ultrasound absorption, tissue heating and post-treatment processes of clearing tissue debris. It is unclear whether the hyaline degeneration observed in case 1 was preexisting. Case 4 had exceedingly high cellularity and perfusion, which explains both the poor heating and rapid tissue healing post-treatment.

Regions of non-organized coagulative necrosis (cases 3 and 5) are readily explained as remnants of the original tissue architecture. These findings are compatible with either ischemia or thermal coagulation necrosis as the primary processes, although thermal fixation cannot be ruled out. Hematoidin deposits and CD31+ remnants of the endothelium confirm that the remains are a vestige of the original tissue architecture.

Regions of dense scarred tissue are best explained by the formation of new scar tissue post-treatment surrounding the treated central area. This is supported by the high degree of organization in the region. The presence of Mib-1+ and MPP-2+ cells is compatible with metabolic activity, although perfusion of blood vessels was only observed in case 7. The Herovici staining of the region did not differ from that of other areas, indicating similar maturity. Scar formation could explain the observed post-treatment leiomyoma growth, at least in some cases. As an alternative hypothesis, these regions could represent the original tissue that has undergone necrosis, from which all other tissue components besides extracellular collagen have been cleaned by immunological processes. However, the high degree of collagen fiber organization and the absence of hematoidin deposits do not support this hypothesis.

At the boundaries of collagenous and leiomyoma tissue, no signs of active immunological reaction or collagen processing were observed. Possibly, such processes existed post-treatment, but had reached a steady state before the samples were obtained.

Our study is limited by the fact that histological findings represent only a single time point for each patient; therefore, processes leading to findings and their causality to the treatment can only be hypothesized. The patient population was intentionally selected based on the need for second-line surgical treatment and was not representative of patients generally. Four of the seven patients used ulipristal acetate, and two of the patients hormonal contraception either before or after HIFU, possibly confounding the results.

Model for volume reduction

Based on literature and our findings, we can hypothesize possible mechanisms behind post-treatment volume reduction and symptom improvement. As the tissue is heated, cell membranes are broken, ECM proteins undergo denaturation,

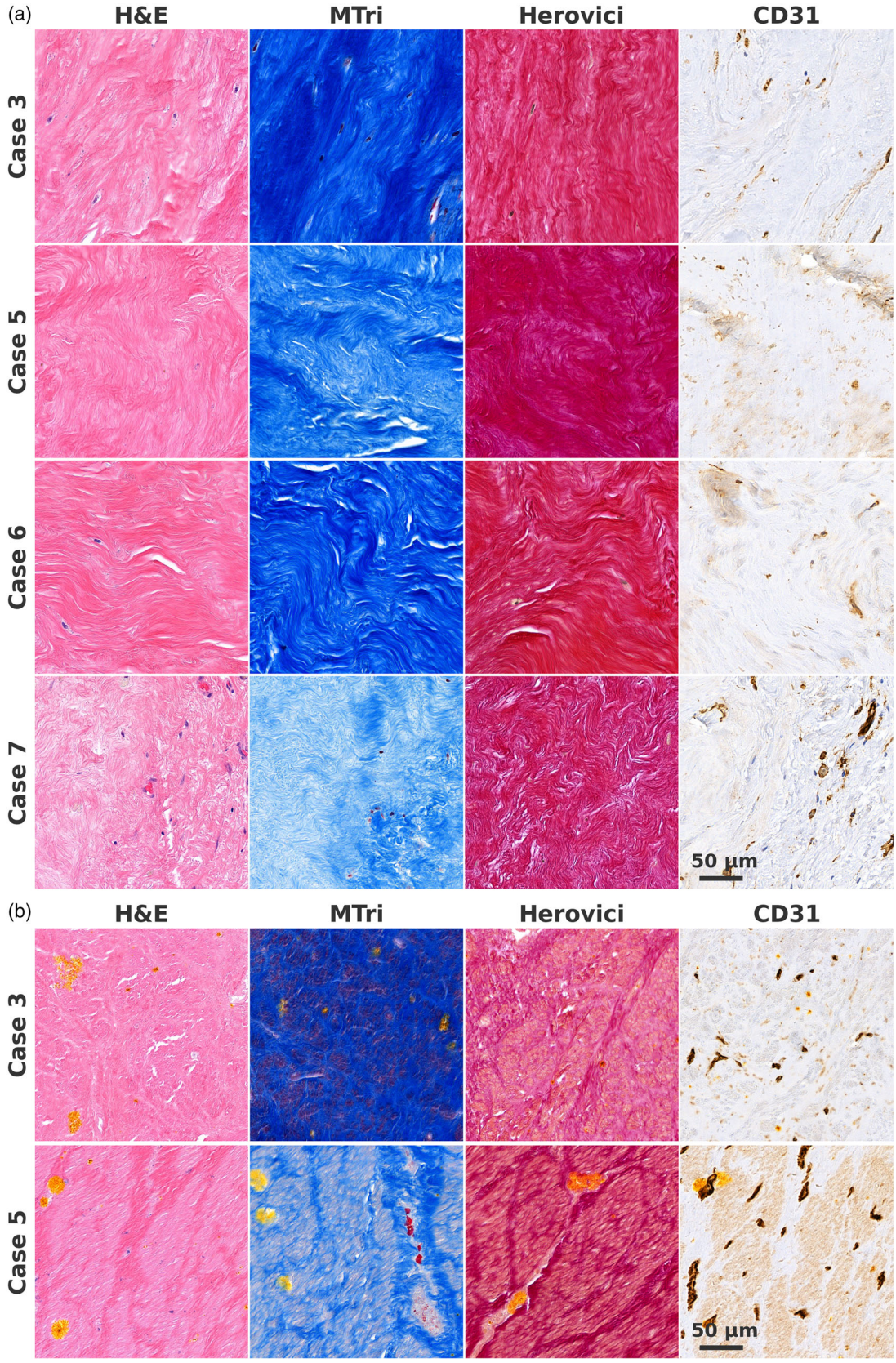

Figure 2. (a) Samples from regions with *dense scarred tissue*. Organized collagen bundles mixed sparsely with basophilic nuclei are seen. Few blood vessels are present in case 7. Scale bar applies for all images. (b) Samples from regions with *non-organized coagulative necrosis*. Original tissue architecture is preserved, empty cell compartments and unorganized collagen bundles are seen. Hematoidin deposits and remnants of blood vessels are present. Scale bar applies for all images.

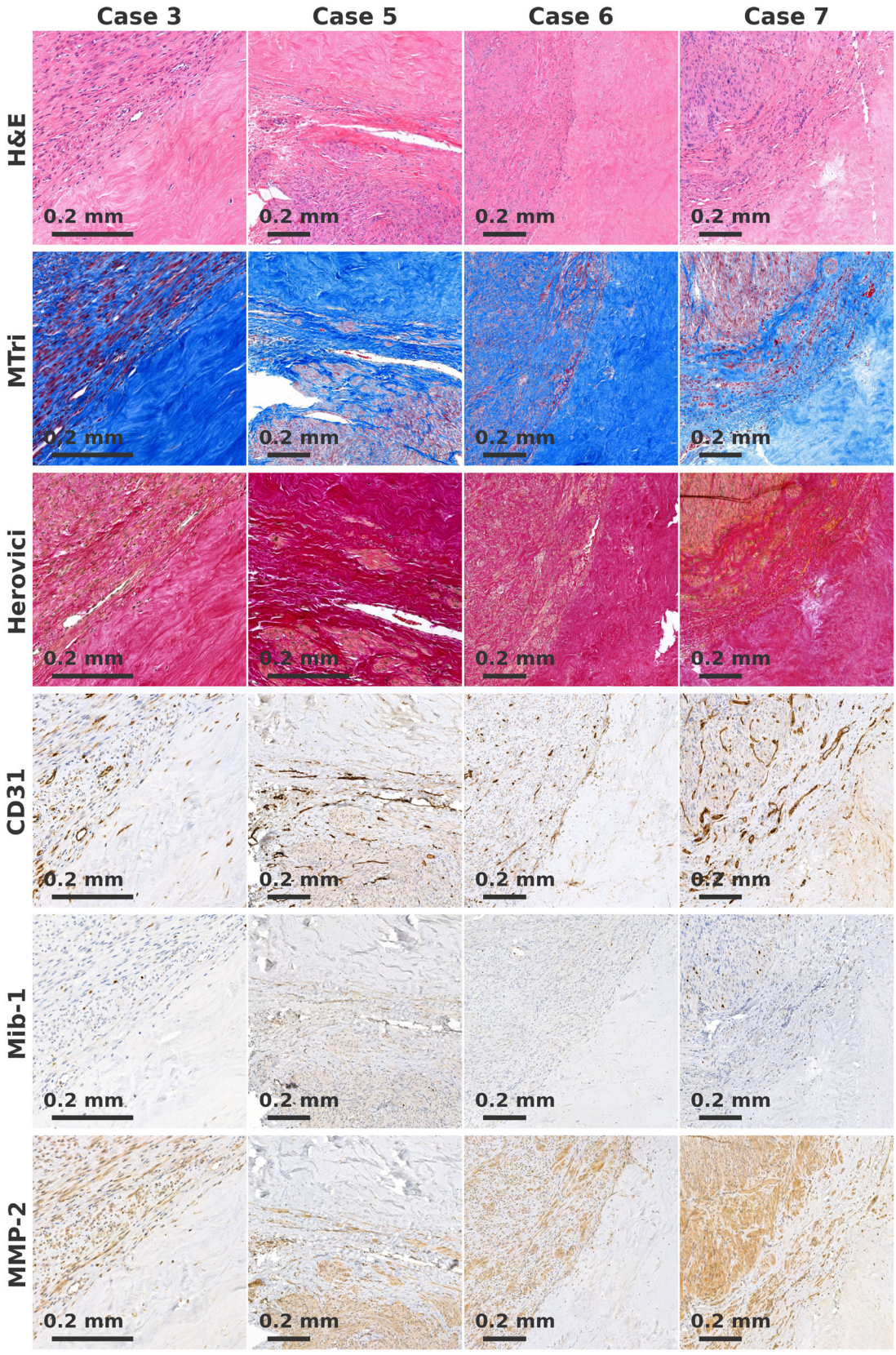

Figure 3. Boundary of remaining leiomyoma tissue and *dense scarred tissue*. No increase of Mib-1+, CD31+ or MMP-2+ cells is seen at the boundary. In Herovici, staining collagen appears mature.

and perfusion ceases. Consequently, the ability of the tissue to retain water diminishes, and some of the initial volume reduction is likely due to the loss of fluid content. Stiffness can be reduced either by the loss of fluid content or the direct thermal changes of tissue components, especially in the ECM. Subsequent enzymatic dismantling of denaturated structures by MMPs and phagocytosis are conceivable, although we did not find any direct evidence for this. In

some cases, dismantling the structures seems impossible, as remnants of the original tissue architecture are seen. This inability could be secondary to the denaturation of the constituent molecules, especially those of the ECM. The formation of dense scarred regions observed here could be an attempt to encapsulate and isolate the remnants of necrotic tissue. There is, however, variation, as evidenced by case 2, where, despite high collagen%, NPV had completely disappeared within six months. In highly cellular leiomyomas with low collagen% (such as case 4), problems with ECM dismantling are likely smaller, and remnants of the SMCs might be removed from the site by phagocytosis, or they could remain *in situ* and transform into (hyaline) degeneration.

In many cases, ischemia extending beyond the heated region has been observed. The processes occurring in such ischemic regions probably differ from those occurring in the actual treatment area, potentially resulting in distinct MRI and histological characteristics. As ischemic regions are known to shrink following UAE therapies, a similar outcome would be expected after HIFU treatment as well.

As previously discussed, shrinkage of the remaining perfused leiomyoma tissue may occur post-treatment. This could be explained by changes in mechanotransduction, hormonal environment or immunological processes affecting untreated regions. On the other hand, an increase in leiomyoma volume could be attributed to the continuous growth of remaining leiomyoma tissue and scarification processes.

Among the weaknesses of this study, low number of patients has to be mentioned. This is primarily due to the low re-intervention rates in our center. Reported cases include only patients where a second-line surgical intervention was required, and therefore are not representative of all HIFU-treated patients. On the other hand, these are the patients we are most interested in since the effect of the primary treatment was not sufficient. Although the number of cases reported here is too low for statistical analysis, we hope that our observations can provide insights to guide future studies.

Acknowledgements

We want to thank the Histocore unit of the University of Turku, Auria Biopankki and the Finnish Institute for Health and Welfare for their assistance with the samples.

Disclosure statement

The authors report there are no competing interests to declare.

Funding

AV reports that his work was partially supported by personal grants from the Radiological Society of Finland and the University of Turku.

Data availability statement

Data are made available on reasonable request.

References

[1] Kim Y-S, Trillaud H, Rhim H, et al. MR thermometry analysis of sonication accuracy and safety margin of volumetric MR imaging-guided high-intensity focused ultrasound ablation of symptomatic uterine fibroids. Radiology. 2012;265(2):627–637. doi: 10.1148/radiol.12111194.

[2] Funaki K, Fukunishi H, Funaki T, et al. Mid-term outcome of magnetic resonance-guided focused ultrasound surgery for uterine myomas: from six to twelve months after volume reduction. J Minim Invasive Gynecol. 2007;14(5):616–621. doi: 10.1016/j.jmig.2007.04.009.

[3] Kim HS, Baik J-H, Pham LD, et al. MR-guided high-intensity focused ultrasound treatment for symptomatic uterine leiomyomata: long-term outcomes. Acad Radiol. 2011;18(8):970–976. doi: 10.1016/j.acra.2011.03.008.

[4] Leppert PC, Baginski T, Prupas C, et al. Comparative ultrastructure of collagen fibrils in uterine leiomyomas and normal myometrium. Fertil Steril. 2004;82:1182–1187. doi: 10.1016/j.fertnstert.2004.04.030.

[5] Tinelli A, Malvasi A, Rahimi S, et al. Myoma pseudocapsule: a distinct endocrino-anatomical entity in gynecological surgery. Gynecol Endocrinol. 2009;25(10):661–667. doi: 10.1080/09513590903015502.

[6] Wei J-J, Zhang X-M, Chiriboga L, et al. Spatial differences in biologic activity of large uterine leiomyomata. Fertil Steril. 2006;85(1):179–187. doi: 10.1016/j.fertnstert.2005.07.1294.

[7] Bourlev V, Pavlovitch S, Stygar D, et al. Different proliferative and apoptotic activity in peripheral versus central parts of human uterine leiomyomas. Gynecol Obstet Invest. 2003;55(4):199–204. doi: 10.1159/000072074.

[8] Fujita M. Histological and biochemical studies of collagen in human uterine leiomyomas. Hokkaido Igaku Zasshi. 1985;60(4):602–615.

[9] Iwahashi M, Muragaki Y, Ikoma M, et al. Immunohistochemical analysis of collagen expression in uterine leiomyomata during the menstrual cycle. Exp Ther Med. 2011;2:287–290.

[10] Wright NT, Humphrey JD. Denaturation of collagen via heating: an irreversible rate process. Annu Rev Biomed Eng. 2002;4:109–128. doi: 10.1146/annurev.bioeng.4.101001.131546.

[11] Fujisawa C, Castellot JJ. Matrix production and remodeling as therapeutic targets for uterine leiomyoma. J Cell Commun Signal. 2014;8(3):179–194. doi: 10.1007/s12079-014-0234-x.

[12] Leppert PC, Jayes FL, Segars JH. The extracellular matrix contributes to mechanotransduction in uterine fibroids. Obstet Gynecol Int. 2014;2014:1–12. doi: 10.1155/2014/783289.

[13] Norian JM, Owen CM, Taboas J, et al. Characterization of tissue biomechanics and mechanical signaling in uterine leiomyoma. Matrix Biol. 2012;31(1):57–65. doi: 10.1016/j.matbio.2011.09.001.

[14] Wolańska M, Sobolewski K, Bańkowski E, et al. Matrix metalloproteinases of human leiomyoma in various stages of tumor growth. Gynecol Obstet Invest. 2004;58(1):14–18. doi: 10.1159/000077177.

[15] Stewart EA, Taran FA, Chen J, et al. Magnetic resonance elastography of uterine leiomyomas: a feasibility study. Fertil Steril. 2011;95(1):281–284. doi: 10.1016/j.fertnstert.2010.06.004.

[16] Hricak H, Tscholakoff D, Heinrichs L, et al. Uterine leiomyomas: correlation of MR, histopathologic findings, and symptoms. Radiology. 1986;158(2):385–391. doi: 10.1148/radiology.158.2.3753623.

[17] Ueda H, Togashi K, Konishi I, et al. Unusual appearances of uterine leiomyomas: MR imaging findings and their histopathologic backgrounds. RadioGraphics. 1999;19(Suppl. 1):S131–S145. doi: 10.1148/radiographics.19.suppl_1.g99oc04s131.

[18] Arleo EK, Schwartz PE, Hui P, et al. Review of leiomyoma variants. AJR Am J Roentgenol. 2015;205(4):912–921. doi: 10.2214/AJR.14.13946.

[19] Cramer SF, Marchetti C, Freedman J, et al. Relationship of myoma cell size and menopausal status in small uterine leiomyomas. Arch Pathol Lab Med. 2000;124(10):1448–1453. doi: 10.5858/2000-124-1448-ROMCSA.

[20] Swe TT, Onitsuka H, Kawamoto K, et al. Uterine leiomyoma: correlation between signal intensity on magnetic resonance imaging and pathologic characteristics. Radiat Med. 1992;10:235–242.
[21] Jondal DE, Wang J, Chen J, et al. Uterine fibroids: correlations between MRI appearance and stiffness via magnetic resonance elastography. Abdom Radiol. 2018;43(6):1456–1463. doi: 10.1007/s00261-017-1314-1.
[22] Zhao W-P, Chen J-Y, Chen W-Z. Effect of biological characteristics of different types of uterine fibroids, as assessed with T2-weighted magnetic resonance imaging, on ultrasound-guided high-intensity focused ultrasound ablation. Ultrasound Med Biol. 2015;41(2):423–431. doi: 10.1016/j.ultrasmedbio.2014.09.022.
[23] Yamashita Y, Torashima M, Takahashi M, et al. Hyperintense uterine leiomyoma at T2-weighted MR imaging: differentiation with dynamic enhanced MR imaging and clinical implications. Radiology. 1993;189(3):721–725. doi: 10.1148/radiology.189.3.8234695.
[24] Oguchi O, Mori A, Kobayashi Y, et al. Prediction of histopathologic features and proliferative activity of uterine leiomyoma by magnetic resonance imaging prior to GnRH analogue therapy: correlation between T2-weighted images and effect of GnRH analogue. J Obstet Gynaecol (Tokyo 1995). 1995;21(2):107–117. doi: 10.1111/j.1447-0756.1995.tb01083.x.
[25] Shimada K, Ohashi I, Kasahara I, et al. Differentiation between completely hyalinized uterine leiomyomas and ordinary leiomyomas: three-phase dynamic magnetic resonance imaging (MRI) vs. diffusion-weighted MRI with very small b-factors. J Magn Reson Imaging. 2004;20(1):97–104. doi: 10.1002/jmri.20063.
[26] Venkatesan AM, Partanen A, Pulanic TK, et al. Magnetic resonance imaging-guided volumetric ablation of symptomatic leiomyomata: correlation of imaging with histology. J Vasc Interv Radiol. 2012;23(6):786–794.e4. doi: 10.1016/j.jvir.2012.02.015.
[27] Stewart EA, Gedroyc WMW, Tempany CMC, et al. Focused ultrasound treatment of uterine fibroid tumors: safety and feasibility of a noninvasive thermoablative technique. Am J Obstet Gynecol. 2003;189(1):48–54. doi: 10.1067/mob.2003.345.
[28] Anttinen M, Yli-Pietilä E, Suomi V, et al. Histopathological evaluation of prostate specimens after thermal ablation may be confounded by the presence of thermally-fixed cells. Int J Hyperthermia. 2019;36:915–925.
[29] Coad JE, Kosari K, Humar A, et al. Radiofrequency ablation causes 'thermal fixation' of hepatocellular carcinoma: a post-liver transplant histopathologic study. Clin Transplant. 2003;17(4):377–384. doi: 10.1034/j.1399-0012.2003.00062.x.
[30] Courivaud F, Kazaryan AM, Lund A, et al. Thermal fixation of swine liver tissue after magnetic resonance-guided high-intensity focused ultrasound ablation. Ultrasound Med Biol. 2014;40(7):1564–1577.
[31] Hennings L, Kaufmann Y, Griffin R, et al. Dead or alive? Autofluorescence distinguishes heat-fixed from viable cells. Int J Hyperthermia. 2009;25(5):355–363. doi: 10.1080/02656730902964357.
[32] Xiong X, Chen F, Chen J, et al. Pathologic evaluation of uterine fibroids ablated with high intensity focused ultrasound. Int J Clin Exp Pathol. 2016;9:6163–6170.
[33] Funaki K, Fukunishi H, Funaki T, et al. Magnetic resonance-guided focused ultrasound surgery for uterine fibroids: relationship between the therapeutic effects and signal intensity of preexisting T2-weighted magnetic resonance images. Am J Obstet Gynecol. 2007;196(2):184.e1–184.e6. doi: 10.1016/j.ajog.2006.08.030.
[34] Kroemer G, Galluzzi L, Vandenabeele P, et al. Classification of cell death. Cell Death Differ. 2009;16(1):3–11. doi: 10.1038/cdd.2008.150.
[35] Coad JE. Thermal fixation: a central outcome of hyperthermic therapies. Proceedings of the Thermal Treatment of Tissue: Energy Delivery and Assessment III. Vol. 5698. International Society for Optics and Photonics; 2005. p. 15–22.
[36] Wall MS, Deng XH, Torzilli PA, et al. Thermal modification of collagen. J Shoulder Elbow Surg. 1999;8(4):339–344. doi: 10.1016/s1058-2746(99)90157-x.
[37] Miles CA, Bailey AJ. Thermal denaturation of collagen revisited. J Chem Sci. 1999;111:71–80.
[38] Voogt MJ, van Stralen M, Ikink ME, et al. Targeted vessel ablation for more efficient magnetic resonance-guided high-intensity focused ultrasound ablation of uterine fibroids. Cardiovasc Intervent Radiol. 2012;35(5):1205–1210. doi: 10.1007/s00270-011-0313-9.
[39] McCluggage WG, Ellis PK, McClure N, et al. Pathologic features of uterine leiomyomas following uterine artery embolization. Int J Gynecol Pathol. 2000;19(4):342–347. doi: 10.1097/00004347-200010000-00008.
[40] Tempany CMC, Stewart EA, McDannold N, et al. MR imaging-guided focused ultrasound surgery of uterine leiomyomas: a feasibility study. Radiology. 2003;226(3):897–905. doi: 10.1148/radiol.2271020395.
[41] Choe YS, Lee WM, Choi JS, et al. Clinical characteristics of patients with leiomyoma who undergo surgery after high intensity focused ultrasound (HIFU). Obstet Gynecol Sci. 2019;62(4):258–263. doi: 10.5468/ogs.2019.62.4.258.
[42] Stewart EA, Gostout B, Rabinovici J, et al. Sustained relief of leiomyoma symptoms by using focused ultrasound surgery. Obstet Gynecol. 2007;110(2 Pt 1):279–287. doi: 10.1097/01.AOG.0000275283.39475.f6.
[43] Bankhead P, Loughrey MB, Fernández JA, et al. QuPath: open source software for digital pathology image analysis. Sci Rep. 2017;7(1):16878. doi: 10.1038/s41598-017-17204-5.
[44] Mindjuk I, Trumm CG, Herzog P, et al. MRI predictors of clinical success in MR-guided focused ultrasound (MRgFUS) treatments of uterine fibroids: results from a single centre. Eur Radiol. 2015;25(5):1317–1328. doi: 10.1007/s00330-014-3538-6.
[45] Suomi V, Viitala A, Sainio T, et al. High-Intensity focused ultrasound therapy in the uterine fibroid: a clinical case study of poor heating efficacy. Annu Int Conf IEEE Eng Med Biol Soc. 2019;2019:2500–2503. doi: 10.1109/EMBC.2019.8857147.
[46] Suomi V, Komar G, Sainio T, et al. Comprehensive feature selection for classifying the treatment outcome of high-intensity ultrasound therapy in uterine fibroids. Sci Rep. 2019;9(1):10907. doi: 10.1038/s41598-019-47484-y.